# Impact of Walking Passengers on the Aerosol Spreading in a Passenger Train

*Laura* Krüger[1], *Robert* Brinkema[1,2], *Daniel* Schiepel[1], and *Daniel* Schmeling[1*]

[1] German Aerospace Center (DLR), Institute of Aerodynamics and Flow Technology, Department Ground Vehicles, Bunsenstraße 10, 37073 Göttingen, Germany
[2] now: LaVision GmbH, Anna-Vandenhoeck-Ring 19, 37081 Göttingen, Germany

**Abstract.** We report on the experimental investigation of the spreading of aerosol particles in a train compartment. For this purpose, a moving thermal manikin is used representing a heat-releasing, standing passenger, which can be moved through the aisle with a peak walking velocity of 1 m/s on a traverse system. The results highlight the impact of the movement by showing high peaks of increased local concentrations on different seats, which are up to nine times higher compared to the average concentration on this seat. Meanwhile the mean concentration in the compartment remains almost constant, whereas on some other seats the average concentration is locally slightly decreased. In general, the movement results in a decrease of the concentration at the highest contaminated seats near the source while increasing the concentration farther away. This effect can be explained by the additional mixing of the air in the cabin. The measurements were performed for different source locations, showing the different spreading behavior originating from aisle and window seats.

## 1 Introduction

The ventilation of passenger train compartments has to meet several standards, e.g., DIN EN 13129 [1] for long-distance trains, to guarantee thermal comfort for the passengers. At the same time, the energy demand of the HVAC system – which is the second largest consumer during a train journey [2] – and the local air quality must be considered. Balancing these three main pillars (thermal comfort, energy demand and air quality) is a challenging task in terms of ventilating passenger trains. Additional boundaries are defined by the geometrical constraints, i.e., available installation areas for air channels and openings as well as by specific operational conditions of the train, such as different climate zones or fast changing conditions such as tunnel passages.

Although the air quality in terms of a sufficient fresh air supply is already defined and has been established in standards for a long time, the Sars-CoV-2 pandemic draw additional attention to this topic. The newly raised questions are: How do exhaled aerosol particles spread in the compartment and in specific how “contaminated” are the other passenger seats?

Furthermore, in cabins and compartments of passenger trains people are frequently moving through the aisle. Besides affecting the general quiescence and the comfort, this movement is also prone to have an influence on the aerosol particle spreading in the cabin. The latter is mainly determined by the superposition of the forced flow generated by the ventilation system and the thermally induced flow by the passengers and has already been investigated in numerous studies. However, in dynamic situations such as the movement of passengers in the aisle, the aerosol particle spreading deviates from the steady-state case.

An analysis of this flow was carried out by Poussou et al. [3] both experimentally and using CFD. A cuboid with dimensions of 0.02 m×0.05 m×0.17 m was used in place of the person in a scaled-down model of an aircraft cabin with a semi-circular cross-section without fittings. A similar investigation for a hospital corridor was undertaken by Wood [4]. In this study, experimental measurements also show that the wake of a person is very similar to that of a cylinder.
The effects of scaling and different model shapes of a moving obstacle/passenger in the aisle of an aircraft cabin were investigated by Mazumdar et al. [5] using CFD with respect to the spreading of SARS in 2003. Their study revealed that a) the scaled water model shows discrepancies of the flow with respect to a full-scale air cabin and b) the shape of the movement influences the contaminant transport. As a consequent continuation of the discussed studies, we developed a movable, full-scale thermal manikin. It comprises all of the above-discussed features: heat release, human-shape, full-scale, movement. It was presented at the Roomvent 2018 conference [6] and is described briefly in section 2.2.

* Corresponding author: daniel.schmeling@dlr.de

## 2 Experimental Setup and Methods

In the following section, we briefly introduce the laboratory, the moving passenger manikin as well as the applied measurement techniques.

### 2.1 Generic Train Laboratory (GZG)

The study was conducted in a generic laboratory, representing the lower cabin of the DLR's next generation train (NGT), see Fig. 1. The inner dimensions of the compartment are 6.0 x 2.88 x 1.95 $m^3$ (length x width x height) and it is equipped with 24 seats. Thermal manikins are used to simulate the blockage and heat release of real passengers.

**Fig. 1.** View in the generic train laboratory fully equipped with thermal manikins.

The heating/ventilation/air-conditioning (HVAC) unit of the GZG is realized using a stationary, high-precision HVAC system, which guarantees well-defined and precise supply air conditions with temperature and air flow rate fluctuations as low as 0.1 K and 10 l/s, respectively., The latter corresponds to an accuracy of approximately 4.3% with regard to the absolute supply air volume flow rate.
The installed ventilation concept during the presented measurements is depicted in Fig. 2.

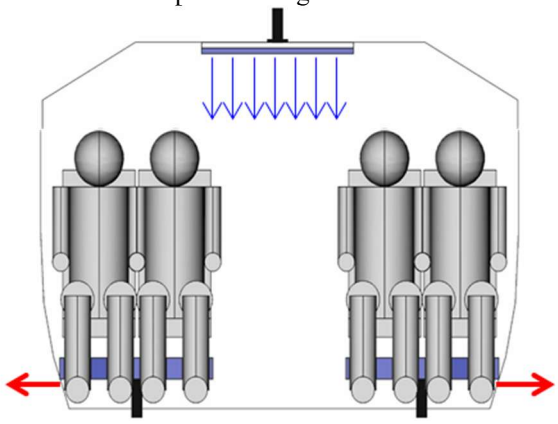

**Fig. 2.** Sketch of the installed ventilation concept.

In previous investigations within the GZG, we analyzed different ventilation concepts [7, 8], individual infrared (IR) heating elements [9] and aerosol spreading for different ventilation concepts [10].

### 2.2 Walking Thermal Manikin

In order to study the effects of moving thermal loads, a controllable thermal manikin on a traverse system was developed by Meyenberg [11]. This system comprises a traverse stage with additional load-bearing capacity, a pre-configured control system for the stepping motor and a standing thermal manikin.
All body parts of the standing thermal manikin except for the legs – which are made of polypropylene pipes with aluminum profiles inside – consist of a foam core (see Fig. 3). This inner structure is wrapped with a heating wire and a thin layer of black painted, high-heat conductivity material. As a result, the manikin provides a spatially homogeneous heat flux density, with increased values in the head region. More details can be found in [6] and [11].
The length of the traverse systems spans the whole 6 m length of the generic train compartment. Hence, a movement of the "walking passenger" through the entire compartment can be simulated. The velocity of the moving manikin was set to 0.6 m/s during the investigated runs and the sensible heat was kept at a constant level of 100 W.

**Fig. 3.** Image of the walking thermal manikin in the generic train compartment.

### 2.3 Measurement Techniques

The experimental analysis of the aerosol spreading comprises three main stages: the generation of the aerosol particles, the detection of the aerosol particles and the evaluation of the measured local aerosol particle concentrations (for details see [12]).

#### *2.3.1 Aerosol Generation*

The aerosol generator consists of an airbrush pistol used to disperse a constant mist of artificial saliva (mixed in accordance with NRF 7.5, receipt see [12]). After the initial generation, the particles are guided through a settling chamber. The setup is designed in such way that the particles already have an age of more than one minute before being released into the cabin, i.e., all evaporation processes are expected to be finished, and

pure dry particles are released. The particle size distribution of the generated particles shows that particles with diameters smaller than 2.5 µm are produced corresponding to normal breathing, for example. The aerosol particles are released into the cabin using a generic face – also known from first aid courses – which is attached to the head of one of the thermal manikins in the compartment, see Fig. 4.

### *2.3.2 Aerosol Detection*

For the acquisition of the local aerosol concentrations in the breathing zones of all passengers, low-cost particulate matter sensors (Sensirion SPS30) are used, ensuring an accuracy of 20 #/cm$^3$ or 10% of the measured value (whatever is larger). The sensors are mounted in the face area of all seated thermal manikins, and thus the local aerosol concentration can be recorded at a sample rate of approx. 0.9 Hz in our setup. The data acquisition is realized using the mobile measurement system of the DLR [13].

**Fig. 4.** Aerosol-exhaling thermal passenger manikin and particle concentration sensors in the breathing zones of all other passengers.

### *2.3.3 Evaluation Process*

The measurements are performed until a quasi-stationary local aerosol particle concentration is reached. The average values for this quasi-stationary period, i.e., 300 s before switching off the aerosol source (see dashed lines in Fig. 6), are calculated for all seats.
To determine the amount of potentially 'inhaled' aerosols, the locally measured equilibrium-state particle concentrations [1/cm$^3$] are multiplied by the typical human tidal breathing volume and by the typical breathing frequency resulting in the number of 'inhaled' particles per minute ($\dot{N}_{seat}$). As our source produces more aerosol particles compared to a human, we calculate the 'inhalation fraction' $f_N = \dot{N}_{seat}/\dot{N}_{source}$, representing the amount of inhaled compared to the amount of exhaled aerosol particles.

## 3 Results

Figure 5 shows a snap-shot of a laser-smoke visualization recorded in a horizontal plane at hip height of the moving manikin. It depicts the wake region behind the moving thermal manikin. The formation of a vortex pair is clearly visible. These vortices induce a flow from the sitting passengers into the aisle. Furthermore, they are attached to the moving manikin and thus, possible contaminants released by a sitting passenger are transported through the passenger compartment. Additionally, the movement of the thermal manikin leads to increased flow velocities in the area of the seated passengers. This induced draft is prone to be comfort-critical.

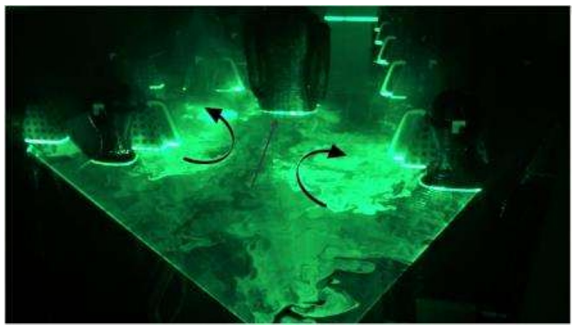

**Fig. 5.** Laser-smoke visualization of the wake downstream of the walking passenger manikin.

### 3.1 Local Particle Concentration

In the first main section of the results chapter, we analyze the local particle concentrations for a selected seat. This is followed by an evaluation of the spatial aerosol particle spreading in the compartment in section 3.2.
Figure 6 presents the local aerosol particle concentrations on a fixed seat, one seat row behind the aerosol source for the cases without (top) and with (bottom) movement of the walking thermal manikin. The aerosol particle source was started at t = 0 s and stopped at t = 2400 s (vertical dashed line), while the manikin was continuously moving forwards and backwards in the aisle for the whole measurement run for cases with movement. The graphs show the local particle concentration as #/cm$^3$ as a function of time for three different particle size bins: 0.3 – 1.0 µm (green), 1.0 – 2.5 µm (blue) and the sum of both 0.3 – 2.5 µm (red). The dashed horizontal lines at 700 #/cm$^3$ are a guide to the eye for a better comparison of the two figures.
The first thing to note is that the majority of the particles have diameters smaller than 1.0 µm. Here, the local number concentrations of the smaller particles are approximately one magnitude higher compared to the larger particles: $N_{0.3-1.0} \approx 700\ \#/cm^3$ and $N_{1.0-2.5} \approx 70\ \#/cm^3$. The second point to note is that the local concentration reaches stable levels after approximately 300 s. That means, about 5 min after the start of the aerosol particle source, a balance between newly produced particles and those removed by the ventilation system is reached. Furthermore, even under stable conditions without movement of the manikin, see Figure 6 (top) for t > 300 s, fluctuations of the local concentrations are observed. These are caused by fluctuations of the airflow, which is a superposition of the forced ventilation airflow and the thermal convection induced by the warm passenger manikins. As a consequence, the airflow, which is responsible for

the transport of the exhaled aerosol particles to the other passengers, starts to fluctuate and leads to more and less high concentrations in the breathing zones of the other passengers. The comparison of the cases with and without movement of the thermal passenger manikin in the aisle reveals similar average values. Hence, the additional movement in the aisle does not change the average load on this selected seat. However, we find much stronger fluctuations in the case with movement. Here, peak values of up to 1200 #/cm$^3$ are recorded reflecting the impact of the movement on the airflow fluctuations and consequently also on the fluctuations of the aerosol transport.

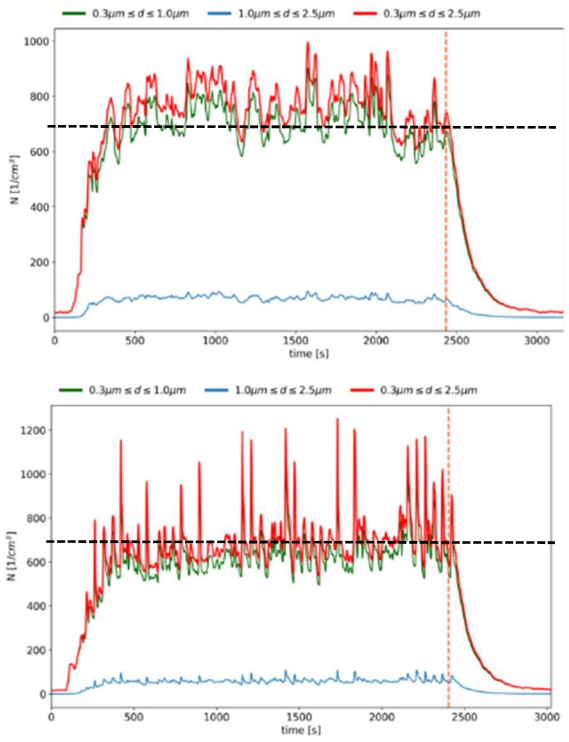


**Fig. 6.** Local particle concentration as a function of time (aerosol exhalation active between t=0 and t=2400 s). Top: without movement, bottom: with movement in the aisle. Dashed horizontal line at N = 700 #/cm$^3$.

### 3.2 Source on a Window Seat

After the brief discussion of the time-dependent aerosol concentration we will now focus on the local time-averaged aerosol concentration in the breathing zones of the passengers in terms of the inhalation fraction. The average values for this quasi-stationary period, i.e., 300 s before switching off the aerosol source (see dashed lines in Fig. 6), are calculated for all seats.

Figure 7 presents the aerosol spreading originating from one window seat, marked with an “S”, for the case without (top) and with (bottom) movement. The existence of the movement of the manikin is also depicted by additional arrows in the aisle. The results are shown in terms of the inhalation fraction, see section 2.3.3., as color code.

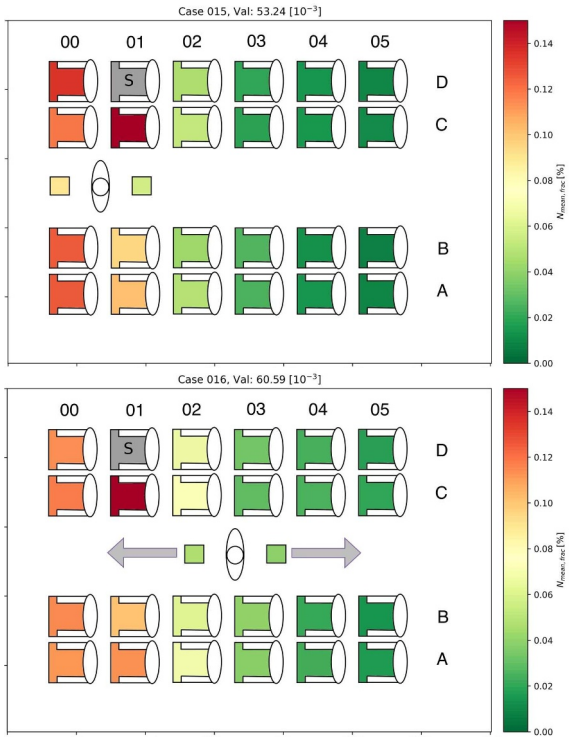


**Fig. 7.** Time-averaged local aerosol concentrations originating from a window seat, marked as “S”, depicted in terms of the inhalation fraction for the case without (top) and with (bottom) movement.

The results reveal, as expected, that the inhalation fraction decreases with increasing distance from the source, i.e., going farther to the rear of the compartment. Furthermore, the aerosol particles spread mostly one row to the front and also towards the other side of the aisle. The rearward transport of the aerosol particles is much weaker. The highest contamination is found for both cases on the direct neighboring seat.

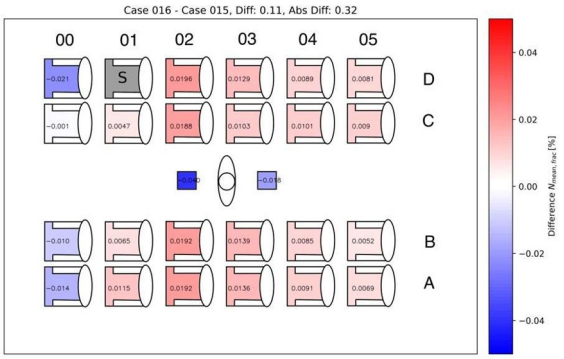


**Fig. 8.** Differences of the inhalation fraction between the cases with and without movement originating from a window seat. Red and blue color codes correspond to higher and lower values in the case with movement, respectively.

For the comparison of the two cases, Figure 8 presents the differences of the local inhalation fractions. Here, a red color code corresponds to higher values for the case with movement and a blue color code vice versa. The main finding is that the movement of the manikin in the aisle results in many seats with increased contamination,

while it is only reduced on very few seats. Reduced values are only found in the first row, i.e., row 00. In front of the aerosol source the movement increased the local contamination on all other seats. It should be noted that these seats, together with row two, revealed the highest local contaminations, see previous figures. This can be explained by the increased mixing of the air in the compartment. This increased mixing leads to an increased aerosol particle transport from the highly contaminated seats in the front of the compartment towards the rear. The highest increase is found in row 02.

### 3.3 Source on an Aisle Seat

In section 3.3 we the same scenario as described in section 3.2 is evaluated but for a different aerosol source location.
Figure 9 presents the aerosol spreading originating from one aisle seat, marked with an "S", for the case without (top) and with (bottom) movement. The existence of the movement of the manikin is also depicted by additional arrows in the aisle. The results are shown in terms of the inhalation fraction, see section 2.3.3., as color code.

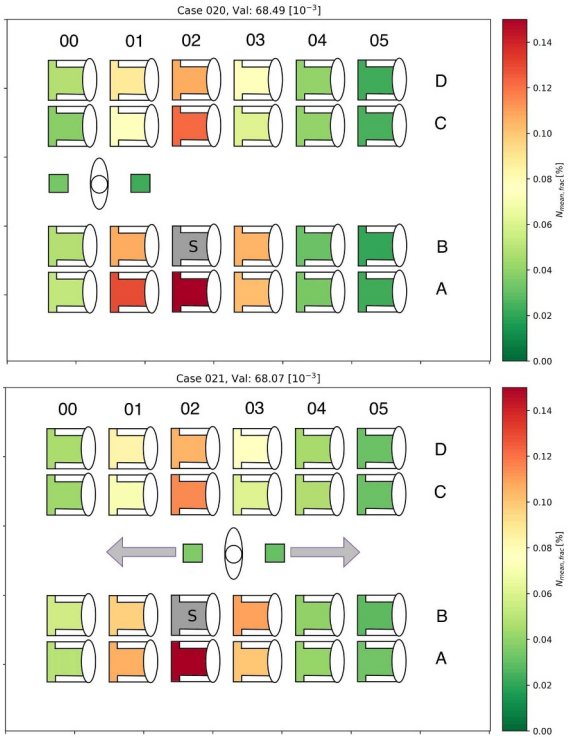


**Fig. 9.** Time-averaged local aerosol concentrations originating from an aisle seat, marked as "S", depicted in terms of the inhalation fraction for the case without (top) and with (bottom) movement.

For both cases, without (top) and with (bottom) movement, we find the highest inhalation fractions, as expected, on the direct neighboring seat, i.e., seat 02A. Increased values with $f_N = 0.10\%$, i.e., orange to red, are found in the adjacent rows and in the same row on the other side of the aisle. The inhalation fractions in the first and in the last two rows are rather low, shown as green values in the figures. In contrast to the case with the source on a window seat one row farther in front, see Figure 7, no significant changes for the cases with and without movement are found.
This finding is also confirmed by the difference map shown in Figure 10, which compares the cases with and without movement for the source on the aisle seat.

This representation reveals that the additional movement in the aisle decreases the inhalation fraction in the vicinity of the source, i.e., on the seats with the highest contamination, while it slightly increases the inhalation fraction in the rear of the compartment and on the two aisle seats in the front row. However, except for the directly neighboring seat (02A) and for the window seat in the row in front (01A), the changes are rather neglectable. A change of the local inhalation fraction larger than 0.01% was only found in these two highest contaminated seats.

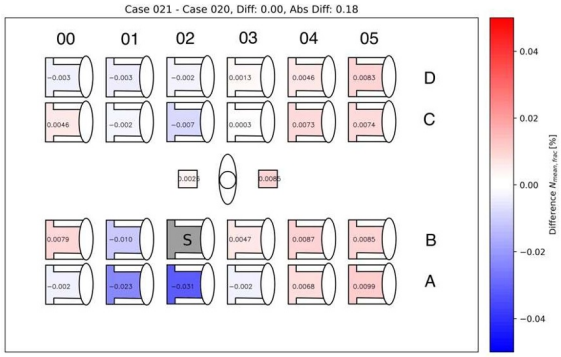


**Fig. 10.** Differences of the inhalation fraction between the cases with and without movement originating from an aisle seat. Red and blue color codes correspond to higher and lower values in the case with movement, respectively.

## 4 Discussion

Before starting the discussion of the results, we want to briefly compare the investigated geometry and set-up with a real-word scenario. Two main points should be reflected: a) the geometry of the investigated train laboratory corresponds to the lower deck of a double-deck passenger train with a typical air flow concepts for cooling conditions. For different geometries, e.g., seating configurations, an increased ceiling height or other ventilation configurations, locally different results are expected. b) the movement velocity of the manikin in the aisle was chosen to 0.6 m/s (≈2.2 km/h) corresponds to slow walking, which is estimated for a moving passenger in the aisle, e.g., going to the restrooms or the restaurant car. Regarding b) we expect only smaller deviation to typical real word conditions, see also reported maximum velocity of boarding passengers in an aircraft aisle of 0.8 m/s [14], while regarding a) we expect a stronger impact of the different ventilation configurations on the local spreading especially regarding the influence of the source location. However, regarding the influence of the movement in the aisle, we expect that the results are generally transferable to real-world applications.

For a comparing discussion of the four investigated cases – source on a window or aisle seat and with or without additional movement of the walking thermal passenger manikin in the aisle – we evaluated the mean aerosol inhalation fraction averaged over all seats as well as the number of seats with values above a certain threshold of the inhalation fraction. It should be noted that the threshold values are chosen arbitrarily and are not linked to, e.g., a certain risk of infection. The results are summarized in Table 1.

**Tab. 1:** Comparison of different configurations: source on a window seat (D01) or aisle seat (B02) as well as with or without movement in the aisle.

| Source | Move-ment | $\langle f_N \rangle$ $[10^{-3}]$ | Number of seats with $f_N$ $> 0.02$ | $> 0.05$ | $> 0.10$ |
|---|---|---|---|---|---|
| D01 | no | 53.2 | 13 | 8 | 6 |
| D01 | yes | 60.6 | 19 | 11 | 7 |
| B02 | no | 68.5 | 22 | 12 | 7 |
| B02 | yes | 68.1 | 23 | 12 | 6 |

The results reveal that the average inhalation fraction increases for the cases with additional movement compared to the cases without movement of the manikin. Further, it also increases when the source is located on an aisle seat compared to a window seat. It must be noted that the row of the source was also changed, which could also have an effect on the average spreading, i.e., the increased values could also be a result of the source being closer to the center of the compartment compared to the source located in the front of the compartment.
Regarding the number of seats with values exceeding a certain threshold, the previous findings are confirmed. We found that for the case with the source on the aisle seat B02, (almost) all other seats reveal an inhalation fraction above 0.02%. In contrast, for the aerosol source positioned on seat D01, only 19 or 13 seats reach inhalation fractions higher than 0.02% with and without movement, respectively. In this case, the effect of movement is evident and results in a significantly increased particle spreading.
Finally, we briefly sketch some possible implications of these findings for public health guidelines. Firstly, a reduction of movement in the aisle could be requested during pandemic situations, which would reduce the average concentration in the breathing zones of the passengers and also. To fully address this point, a further measurement campaign with different movement velocities would also be helpful. Secondly, for the chosen configuration in our laboratory, a recommendation to place potentially sick passengers on the window rather than on the aisle seats would also reduce the spreading of contaminants to the breathing zones of the other passengers. At this point it should be noted that the latter result will strongly depend on the train configuration and in specific on the installed ventilation concept. For the design of train ventilation systems ongoing studies on different air flow configurations will help to draw further implication regarding benefits and drawbacks of singe concepts in terms of aerosol particle spreading.

## 5 Conclusions and Outlook

This paper presents an experimental investigation on aerosol particle spreading in terms of different source locations, i.e., different index passengers, and regarding the influence of additional movement in the aisle. Therefore, a 24-seat generic train compartment was fully equipped with thermal manikins including local aerosol particle concentration measurement sensors in the breathing zones. A standing thermal manikin on a traverse system was used to simulate the passengers walking up and down the aisle.
The results revealed that the aerosol particle spreading originating from an aisle seat in the central region of the compartment is stronger compared to a window seat in the front region of the compartment. Furthermore, we found that the additional movement in the aisle has only a minor influence on the particle spreading when the index passenger is seated on the aisle seat in the central part of the compartment. Only the direct neighboring seats are significantly influenced by the movement in the aisle, showing lower peak values in the case with the movement.
In contrast, for the aerosol source positioned on the window seat in the front part of the compartment, we found a strong increase of the aerosol particle spreading caused by the additional movement in the aisle. Both average inhalation in the compartment and the number of seats with concentration values above certain thresholds increased with the movement.
Furthermore, we found strong peaks of the local aerosol concentration caused by the additional movement in the aisle, which can be attributed to the additional air mixing and entrainment in the wake region of the walking manikin.

## Acknowledgements and Funding

The authors would like to thank André Volkmann and Felix Werner for the technical assistance of the set-up and the measurements. Further, the authors would like to thank Annika Köhne for proof-reading the manuscript.
This work was performed partially within the framework of the Rolling Stock (RoSto) project of the German Aerospace Center and partially supported by the Initiative and Networking Fund of the Helmholtz Association of German Research Centres (HGF) under the CORAERO project (KA1-Co-06).


## References

1. DIN EN 13129, “Railway applications – Air conditioning for main line rolling stock – Comfort parameters and type tests; German version“, Beuth, 2016.
2. I. Ebinger, J. Morgenstern, “Klimatisierung von Schienenfahrzeugen“ (in German), VDE / Beuth (2021).

3. S. B. Poussou, S. Mazumdar, M. W. Plesniak, P. E. Sojka, Q. Chen : "Flow and contaminant transport in an airliner cabin induced by a moving body: Model experiments and CFD predictions". Atmospheric Environment, **44**, 2830-2839 (2010). doi:10.1016/j.atmosenv.2010.04.053.
4. R. Wood: "Experimental and theoretical studies of contaminant transport due to human movement in a hospital corridor". PhD thesis, University of Leeds, UK (2015).
5. S. Mazumdar, S. Poussou, C.-H. Lin, S.S . Isukapalli, M.W. Plesniak, Q. Chen: "The impact of scaling and body movement on contaminant transport in airliner cabins". Atmospheric Environment, 45(33), pp 6019-6028 (2011). doi: 10.1016/j.atmosenv.2011.07.049
6. S. Winter, M- Meyenberg, D. Schmeling: "A moving thermal manikin for the simulation of walking passengers in aircraft or trains", In Proceedings of the Roomvent and Ventilation Conference, 2018, pp 1097-1102, Espoo, Finland, 02.-05.06.-2018.
7. D. Schmeling, A. Volkmann: "On the experimental investigation of novel low-momentum ventilation concepts for cooling operation in a train compartment". Building and Environment **182**, 107116 (2020). doi: 10.1016/j.buildenv.2020.107116
8. O. Zierke, P. Goerke, J. Maier, H.-J. Hörmann: "Effects of personal control on thermal comfort: A psychological effect or just the "right" temperature? ", Energy and Buildings **295,** 113334 (2023) doi :10.1016/j.enbuild.2023.113334.
9. D. Schmeling, H.-J. Hörmann, A. Volkmann, P. Goerke: "Impact of Local Comfort Zones in Long-Distance Rolling Stock on Objective and Subjective Thermal Comfort Rating", In Proceedings of the 12th World Congress on Railway Research, 2019.
10. D. Schiepel, A. Volkmann, D. Schmeling: "Influence of the airflow concept on the aerosol spreading in a generic train compartment", in Proceedings of Transport Research Arena (TRA) 2024, Dublin, Ireland, 15.-18.04.2024.
11. M. Meyenberg : "Development of an independent control unit for pre-configured control of a movable heat source". (In German) Bachelor thesis. University of Applied Science and Arts (HAWK), Faculty of Natural Sciences and Technology, Göttingen, Germany (2017).
12. D. Schmeling, A. Shishkin, D. Schiepel, C. Wagner: "Numerical and experimental study of aerosol dispersion in the Do728 aircraft cabin". CEAS Aeronautical Journal **14**, 509-526 (2023). doi: 10.1007/s13272-023-00644-3.
13. K.A. Niehaus, A. Westhoff: "An open-source data acquisition system for laboratory and industrial scale applications". Measurement Science & Technology, **34,** 027001 (2023). doi: 10.1088/1361-6501/ac9994
14. M. Schultz: "Fast Aircraft Turnaround Enabled by Reliable Passenger Boarding". Aerospace, **5**, 8 (2018). doi: 10.3390/aerospace5010008